

3 TECHNICAL BASIS FOR AMBIENT SEEPAGE FACTORS IN TPA VERSION 5.1

In this section, the effects of the natural flow zones and components of the engineered barrier system (EBS) on the ambient seepage are discussed. The discussion will focus on three areas: (i) the fractured unsaturated flow zone above the drift wall in which the flow rate is affected by the structural features such as faults and fractures; (ii) the flow zone in the close vicinity of the drift wall across which the changes in the flow rate are controlled by the capillary barrier imposed by the drift opening; and (iii) the rubble flow zone above the drip shield in degraded drifts.

The seepage factors that represent the changes in the flux rate in different flow zones may be constant values, time-series data, or internally computed time-variant parameters in Total-system Performance Assessment (TPA) Version 5.1. They are empirical parameters. The values, or ranges of values, for each parameter were quantified based on independent experimental observations, process-level numerical analyses, and staff judgment. Correlation among the seepage factors was explored to confine parameter uncertainties in TPA simulations.

3.1 WastePackageFlowMultiplicationFactor and SubAreaWetFraction

Any water entering drifts at Yucca Mountain will likely result from flow in fractures. Because of the strong capillary forces in the small pores of welded tuffs at the drift wall, negligible water is expected to enter the drifts from pores in the welded tuffs unless the water pressure in pores approaches the atmospheric condition. Accordingly, the conceptual model for the seepage process neglects the water in the matrix and focuses on the contribution of the fractures.

The welded units at Yucca Mountain have far more capacity in the fracture system to carry flow than is likely to occur under natural infiltration. For example, median fracture hydraulic conductivity ranges from 4.9×10^3 to 3×10^6 mm/yr [16 to 9800 ft/yr] in rock surrounding subsurface niches and alcoves, estimated using air permeability tests (Bechtel SAIC Company, LLC, 2004), which is approximately 2 to 5 orders of magnitude greater than estimated million-year-average mean annual infiltration fluxes (Stothoff and Walter, 2007). Accordingly, most fractures are expected to be at least partially dry, or unsaturated, although some fractures may be completely saturated. Under this over-capacity situation, the interplay between fracture network geometry, capillary forces, and the supply of water to the system will mediate between those fractures carrying liquid water and those fractures remaining dry. Capillary forces are inversely proportional to the radius of curvature of the water/air interface, which is largely determined by the fracture aperture, thus capillary forces preferentially draw water into the smallest apertures first if water is available, and the importance of capillary forces relative to gravity rapidly decreases with increasing fracture aperture. On the other hand, the volume of flow is proportional to the cube of the aperture for a given gradient in potential. In gravity-dominated flow within a fracture, flow moves in the steepest direction without a tendency to move laterally unless flow is restricted by some barrier. Only seepage occurring above the waste package itself can drip on the waste package. The geometry of this potential drip zone is long and narrow, because the waste packages will be laid end-to-end in the drift. The essentially one-dimensional long and narrow geometry of the potential drip zone suggests that a one-dimensional analysis reasonably describes seepage locations, with seepage occurring at discrete intervals along the drift. This assumption is appropriate because waste packages, with

a nominal length of 5.165 m [16.9 ft], are longer than most fracture traces, so that few seeping fractures (active fractures) will drip on more than one waste package. For example, half of the fractures in the upper lithophysal (Ttptul) and middle nonlithophysal (Ttptmn) units of the Topopah Springs formation mapped during the ESF fracture line survey discussed later in this section, in sections where all fractures with trace lengths of at least 0.3 m [1 ft] were mapped, are less than 1.3 m [4.3 ft] in length and 95 percent are shorter than a waste package.

With the assumption of a one-dimensional analysis, two factors are important in describing seeps: (i) the separation between seep locations and (ii) the amount of water flowing in each seep. These factors are strongly inversely related when there is a fixed total flow rate of water. For example, consider two situations where the average separation between seeps differs by a factor of 10. If the same total flow is moving through the system, the flow in the seeps with the large separation, on average, will be 10 times greater than the flow in the seeps with the small separation.

The TPA Version 5.1 uses the related concepts of a SubAreaWetFraction and a WastePackageFlow MultiplicationFactor to describe seeps. The WastePackageFlowMultiplicationFactor characterizes the relative increase in the quantity of water contacting waste packages due to mountain-scale flow convergence and divergence above the drift horizon, and the SubAreaWetFraction characterizes the fraction of waste packages that are contacted by seeps. To date, there is no reported direct observation of drips in the Topopah Springs welded tuff within the Exploratory Studies Facility (ESF)¹ and the Enhanced Characterization of the Repository Block (ECRB)² cross drift at Yucca Mountain. Bulkheads have been emplaced in the ECRB cross drift; but evidence of moisture in the ECRB cross drift has been observed after extended periods with closed bulkheads and no ventilation.³ The anecdotal evidence, in the form of scattered discolored spots and corrosion, may be due to condensation or due to dripping from fractures and anchor bolt cavities. Because direct evidence of dripping is lacking, estimates for these TPA parameters are derived from indirect evidence and interpretive models.

Detailed line surveys in the ESF and ECRB collected intersections of long fractures with the one-dimensional scanline located 0.9 m [3.0 ft] below the left wall spring line (Albin, et al., 1997; Barr, et al., 1996; Beason, et al., 1996; Eatman, et al., 1997; Mongano, et al., 1999). The survey only recorded fractures above a cutoff length of 0.3 m [1 ft] or 1 m [3.3 ft], with the cutoff criterion varying by section. Approximately 15 percent of the total length of emplacement drifts is anticipated to occur within the Ttptmn horizon, with the remainder in the Ttptll (lower lithophysal) horizon. For the purposes of an illustrative analysis, the intersection data from Station 1015.04 to Station 1442.28 in the ECRB cross drift was used to describe the Ttptmn horizon and the intersection data from Station 1445.49 to Station 2324.48 were used to describe the Ttptll horizon; these sections used a cutoff trace length of 1 m [3.3 ft]. Features identified as fractures, shears, faults, vapor phase partings, and cooling joints were considered

¹Exploratory Studies Facility (ESF) is referenced throughout this report; consequently, the acronym ESF will be used.

²Enhanced Characterization of the Repository Block (ECRB) is referenced throughout this report; consequently, the acronym ECRB will be used.

³M. Peters, Yucca Mountain scientific and engineering update, presentation to the Nuclear Waste Technical Review Board, May 9, 2001.

in calculating intersection separation. The mean, median, and standard deviation of the intersection separations are 0.46, 0.32, and 0.45 m [1.5, 1.0, and 1.5 ft], respectively, for the Ttpm and are 2.9, 1.6, and 4.4 m [9.5, 5.2, and 14 ft], respectively, for the Ttpll. These statistics are likely to vary somewhat across the repository footprint due to differences, for example, in ashflow cooling histories and layer thicknesses.

The cumulative distribution of intersection separation is shown for both segments in Figure 3-1, with the length of a waste package indicated for reference. A lognormal distribution for each horizon is also indicated for reference, calculated using the mean and standard deviation of the log-transformed separations. If the remainder of the potential repository has similar fracture separation characteristics, almost every waste package in the Ttpm horizon would have at least one long fracture above it and approximately 80 percent of the waste packages in the Ttpll horizon would have at least one long fracture above it.

There are known biases in measuring fracture trace length and orientation using the detailed line survey methodology (Smart, et al., 2006). For example, the numerous fractures with traces less than 1 m [3.3 ft] in length are not considered. In addition, the ECRB is a near-horizontal tunnel oriented at 229°; therefore, shallowly dipping (i.e., subhorizontal) fractures or fractures nearly parallel to the ECRB (i.e., northeast-southwest striking fractures) are undersampled in this data set. Because seepage is expected to occur primarily in subvertical fractures, the undersampling of subhorizontal fractures in these analyses was considered to be insignificant in estimating SubAreaWetFraction and WastePackageFlowMultiplicationFactor. Smart, et al. (2006) considered biases in the line survey methodology, finding that the major fracture set orientations in the Ttpll do not include a significant proportion of northeast-southwest striking fractures. Further, the ECRB is expected to be nearly parallel to the drift orientations; thus the orientation biases in the ECRB may be similar to the biases in the actual drifts. Accordingly, the intersection data is used directly in the following analysis, with the caveat that the many smaller fractures are not considered.

Not all fractures described in the line survey are expected to seep. Based on field and experimental observations, only a fraction of the connected fractures transmits water in a partially saturated and fractured host rock (Liu and Bodvarsson, 2001; Liu, et al., 2004, 2003; Seol, et al., 2003; Zhou, et al., 2006). These fractures are often termed active fractures. Liu, et al. (1998) used the concept of active fractures to describe the fraction of connected fractures in an unsaturated fractured domain that contributes to fracture flows and used inverse modeling to estimate that approximately 18 to 27 percent of the connected fractures in the Topopah Spring welded unit are active. The potential repository would be located in the Topopah Spring welded unit. The fracture connectedness in the line survey was not evaluated, and the fraction of surveyed fractures that is disconnected is a significant source of uncertainty. Because the line survey only considered fractures with long traces, it is reasonable to expect that many of the surveyed fractures are connected to some extent, if only through myriad unmapped small fractures, but some fraction of the fractures may be disconnected. Accordingly, it is reasonable to expect that the methods of Liu, et al. (1998) would suggest that less than 18 to 27 percent of the mapped fractures would carry water.

A straightforward analysis illustrates the interplay between fracture spacings, the active fracture concept, the SubAreaWetFraction, and the WastePackageFlowMultiplicationFactor. The two lognormal distributions shown in Figure 3-1 are used to describe the fracture spacing statistics along a hypothetical drift. The distributions were used to generate a set of 10⁵ hypothetical

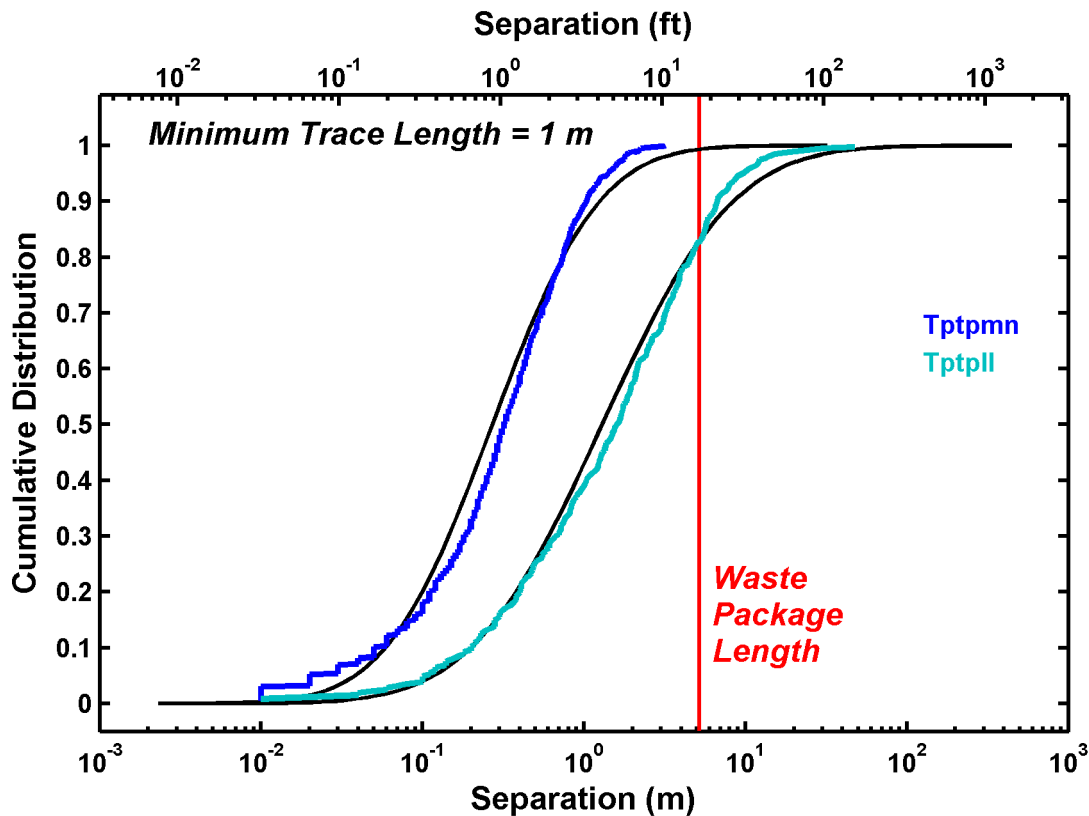


Figure 3-1. Cumulative Distribution of Fracture Separations in the Tptpmn and Tptpll Horizons Determined Using Detailed Line Surveys. Log-Normal Distributions With the Same Mean and Standard Deviation of the Log-Transformed Separations Are Shown for Reference.

fracture spacings for the Tptpmn horizon and another for the Tptpll horizon, assuming for the purposes of illustration that adjacent fracture spacings are uncorrelated. The spacings provided a sequence of fracture locations. A line of waste packages was placed under the fracture sequence; each package was 5.2 m [17 ft] long, and the packages were separated by 0.1 m [3.9 in].

The SubAreaWetFraction is straightforwardly determined by simply counting the number of waste packages with an overlying fracture. Randomly discarding a fraction of the fractures before counting the intersections accounts for the active fracture concept. Figure 3-2(a) demonstrates the SubAreaWetFraction determined as a function of the seeping fracture fraction, which is the fraction of mapped fractures that seep. The seeping fracture fraction and the active fracture fraction are the same if all mapped fractures are connected. The 18- and 27-percent limits suggested by Liu, et al. (1998) are provided in Figure 3-2(a) for visual reference.

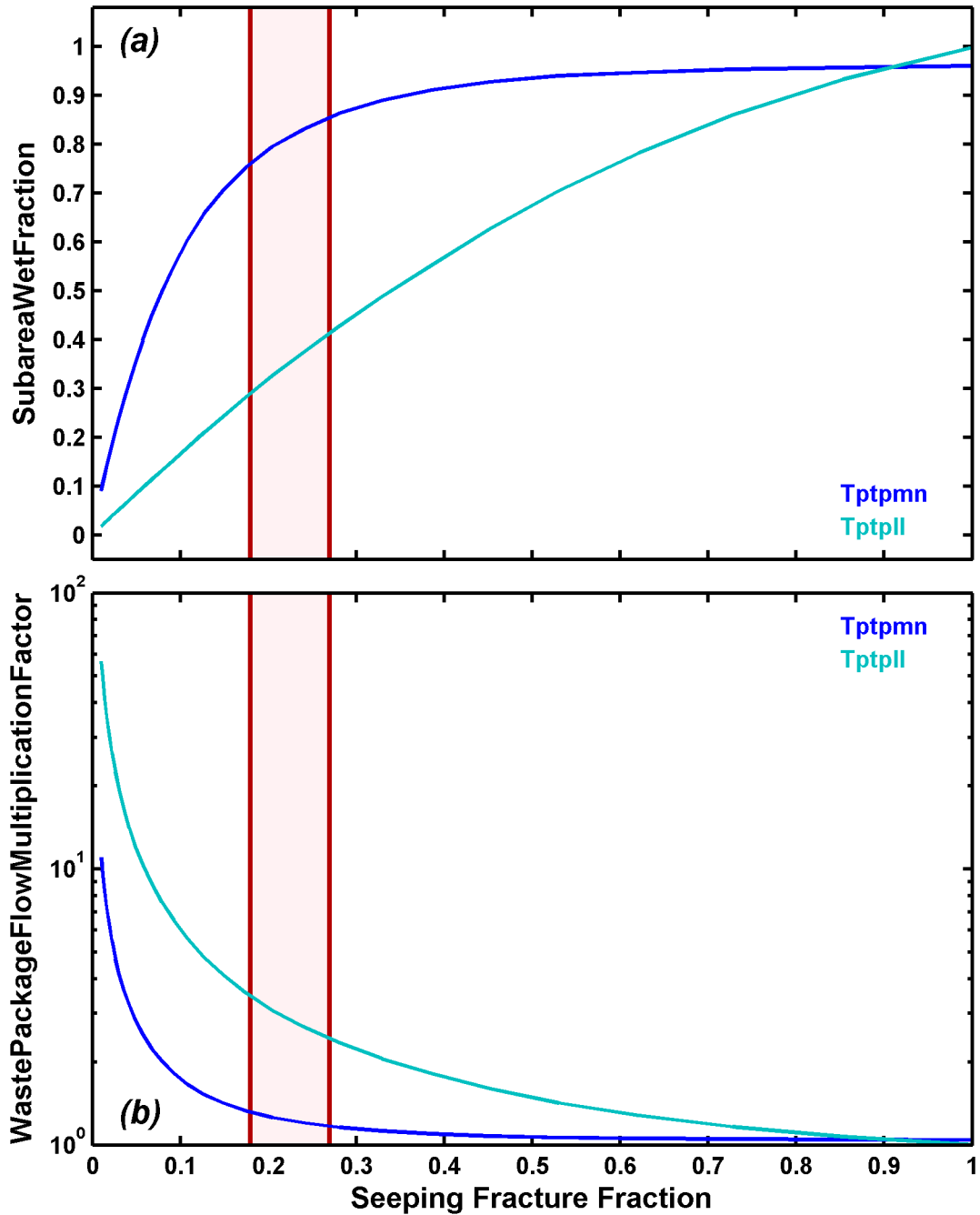


Figure 3-2. (a) SubAreaWetFraction and (b) WastePackageFlowMultiplicationFactor for the Tptpmn and Tptpl Horizons as a Function of Seeping Fracture Fraction. The Range of Active Fracture Fractions Estimated by Liu, et al. (1998) is Shown for Reference. Shaded Areas Correspond to 18 and 27 Percent Limits.

At these limits, the SubAreaWetFraction is approximately 0.75 to 0.9 for the Tptpmn horizon and approximately 0.3 to 0.4 for the Tptpll horizon.

The WastePackageFlowMultiplicationFactor is estimated using the same fracture sets. Each flowing fracture carries all of the water flowing within a “capture zone” or localization (drainage) zone, with the remainder of the capture zone either matrix or dry fractures. In the analysis, each seeping fracture is assigned half of the distance to the next seeping fracture on either side. The WastePackageFlowMultiplicationFactor is calculated by summing the total capture zone length over all seeping fractures that intersect a waste package and dividing by the total length of the waste packages that have a seep above them. Figure 3-2(b) demonstrates the WastePackageFlowMultiplicationFactor determined as a function of the seeping fracture fraction. Again, the 18- and 27 percent limits suggested by Liu, et al. (1998) are provided for visual reference. At these limits, the WastePackageFlowMultiplicationFactor is approximately 1.15 to 1.3 for the Tptpmn horizon and approximately 2.4 to 3.5 for the Tptpll horizon.

Figure 3-2 suggests that, for a given seeping fracture fraction, waste packages in the Tptpmn are more likely to have seeps intersecting them but the amount of water focused onto the waste packages is likely to be smaller relative to waste packages in the Tptpll. Figure 3-3 rearranges the results shown in Figure 3-2 by plotting the WastePackageMultiplicationFactor versus SubAreaWetFraction for specific values of the seeping fracture fraction, indicating that the SubAreaWetFraction and WastePackageMultiplicationFactor are inversely related for both horizons. Note that this inverse relationship implies that the fewer packages contacted by water, the greater the amount of water (on average) contacting each of the wetted waste packages.

The actual distribution of flow in fractures remains uncertain at Yucca Mountain. Niche and alcove experiments have rapidly introduced large volumes of water into the unsaturated zone, with flow characteristics examined for these cases, but it is not clear that these experiments are representative of the low-magnitude, long-duration flows more likely to be typical of Yucca Mountain. These tests exhibited minimal flow entering the cavities, but successive injection tests along horizontal boreholes suggest that seepage patterns may be more closely linked to the character of fractures intersected in the borehole than to diversion by capillarity in the fracture network approaching the niche and alcove settings. In the extreme of fully saturated conditions, fracture network characteristics throughout the network determine the flow pathways. As the network becomes more unsaturated, it is reasonable to expect that the link between fracture network characteristics and flow pathways is increasingly governed by local fracture and intersection characteristics; thus the spatial distribution of the water entering the layer becomes increasingly important.

With this reasoning, the spatial distribution of water-carrying fractures in a highly transmissive, gravity-dominated layer may be largely determined at the upstream end by the spatial patterns of water moving through low-transmissivity upstream layers, with these inherited patterns gradually coalescing into a new characteristic distribution given contact with sufficient numbers of fracture intersections.

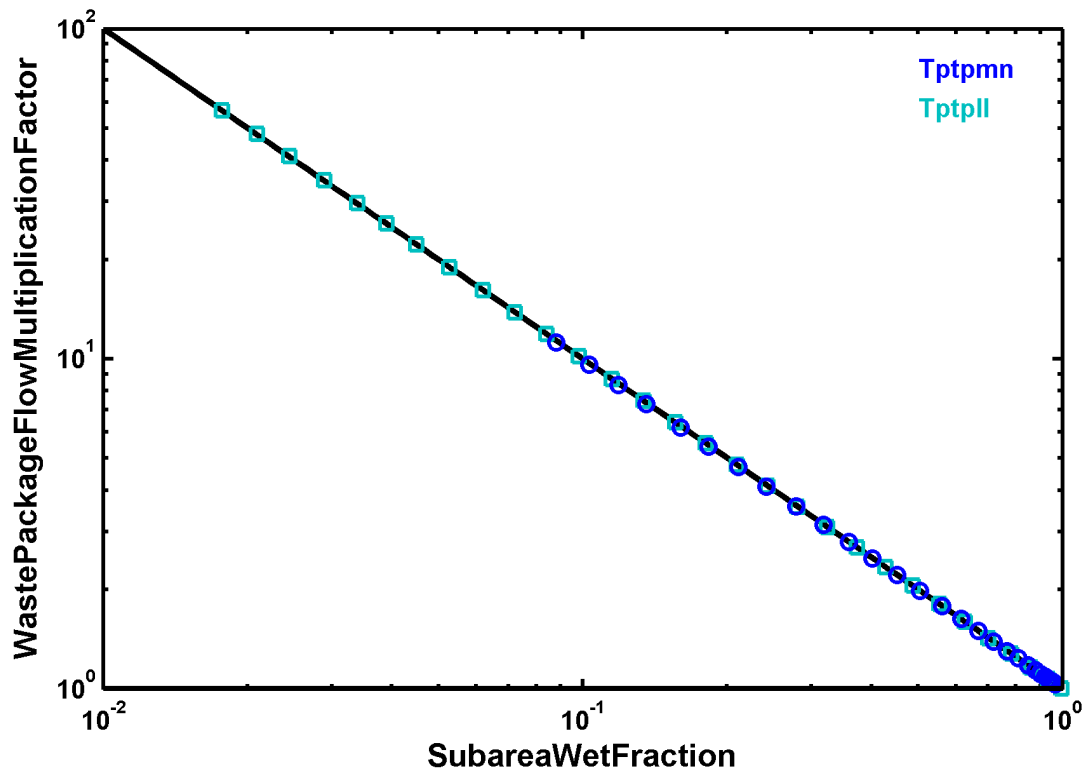


Figure 3-3. SubAreaWetFraction and WastePackageMultiplicationFactor Pairs in the Tptpmn and Tptpll Horizons Given a Seeping Fracture Fraction. The Two Parameters Are Inversely Related.

The Paintbrush Tuff nonwelded unit represents the most significant low-fracture-transmissivity layer at Yucca Mountain, because the matrix is permeable, relatively few discontinuities exist, and capillary forces tend to draw water into the matrix. Data on discontinuity separation is sparse because of the relatively short intervals exposed in the ESF, but it is reasonable to expect that the cumulative distribution of fracture separations would lie to the right of the Tptpll distribution in Figure 3-1. It is likely that the transitions between the overlying welded unit, the nonwelded unit, and the underlying Topopah Spring welded tuff provide a strong patterning to flow at the top of the Topopah Spring welded tuff, and this patterning may not be fully muted at the proposed repository horizon. If the relatively widely separated discontinuities in the nonwelded unit control patterning at the repository horizon, then the seeps may be more widely separated than would be suggested by fracture patterns at the repository horizon. On the other hand, the densely fractured horizons between the nonwelded unit and the Tptpmn may overcome the patterning imposed at the top of the Topopah Spring welded unit. This would imply that the Tptpll unit would have a spatial patterning of seeps at the top of the horizon that is characteristic of the Tptpmn unit. Because there is a relatively short vertical distance from the base of the Tptpmn horizon to drifts in the Tptpll horizon, the characteristic seep separation for

the Tptpll may not be achieved and the seep pattern for the Tptpmn horizon may be a more appropriate description for seeps at the drift horizon in the Tptpll horizon.

Implementation in TPA Version 5.1

Speculation regarding the range of seepage patterns at the repository horizon implies that the SubAreaWetFraction is a fairly uncertain parameter. The upper bound of the range must be close to 1, reflecting the possibility that the characteristic Tptpmn seep characteristics apply in both horizons. The lower bound of the range is less well defined. Staff judgment sets the lower bound of the range to 0.25 for the purposes of TPA analyses, reasonably representing the range of alternatives arising from (i) imprinting from the nonwelded unit, (ii) the low end of the active fracture fraction distribution for the Tptpll horizon, and (iii) an estimate of 0.26 to 0.29 arising from a Monte Carlo analysis considering faults, fracture zones, and shear zones (Center for Nuclear Waste Regulatory Analysis Scientific Notebook 382). A uniform distribution is the maximum entropy distribution for an uncertain parameter with known bounds and without known central tendencies. The seeping fracture fraction is used as the key uncertain parameter, and it is assumed that this parameter is uniformly distributed. In the Tptpll horizon, the SubAreaWetFraction is approximately proportional to the logarithm of the seeping fracture fraction when the seeping fracture fraction is greater than 0.2. Accordingly, a uniform distribution for the seeping fracture fraction implies that the SubAreaWetFraction is log-uniformly distributed. With this rationale, the SubAreaWetFraction parameter in the TPA Version 5.1 code is described as log-uniformly distributed between 0.25 and 1. This parameter is assumed to be held fixed throughout the simulation.

Under the extreme case where the SubAreaWetFraction is 1, the WastePackageFlow MultiplicationFactor must also be 1 to achieve a flow balance. Given this extreme case, the perfect negative correlation between the SubAreaWetFraction and the Waste PackageFlow MultiplicationFactor seen in Figure 3-3 requires that the WastePackageFlowMultiplicationFactor must be log-uniformly distributed between 1 and 4. With this rationale, the TPA parameter WastePackageFlowMultiplicationFactor is described as log-uniformly distributed between 1 and 4, and the two parameters are correlated using the most negative correlation allowed by the TPA Version 5.1.

3.2 Near- and In-drift Flow Diversion, F_{mult}

The flow path of the water near the drift opening is largely determined by the relative strength of gravitational forces exerted by the volume of deep percolating water and the capillary barrier imposed by the drift opening. As the water approaches the drift at a low flow rate, it can be diverted away around the drift opening. However, if the volume and rate of the water in fractures above the drift ceiling are large enough (i.e., high gravitational force of the water), the percolating water may breach the capillary barrier and seep into an emplacement drift. Also, flow regimes such as rivulet and thick film flow may occur, which are much less constrained by capillarity for crossing the drift wall boundary. A flow (seepage) reduction in the vicinity of the drift wall is quantified by a seepage factor, F_{mult} (Figure 2-1). Critical processes responsible for the seepage reduction involve the capillary barrier above the outer walls of the drift imposed by the drift opening and lateral diversion of seeping water in films or rivulets on the wall of the drift.

As the water approaches the drift ceiling, capillarity in the fracture network may divert some of the water laterally around the drift opening. Water that is not diverted may seep from the ceiling

or from protuberances along the drift if the gravitational force is higher than the interfacial tension and capillary strength on the drift wall surface. If the gravitational force of the water is large enough to breach the capillary barrier, but not high enough to drip, seepage can flow as films along the inner walls of the drift and hence may bypass the EBS below. The effects of these two processes, capillary diversion at the drift wall and along-wall seepage, are lumped into a flow reduction factor named F_{mult} in TPA, which varies from 0 to 1. If all percolating water seeps onto rubble or the EBS components, the value of F_{mult} is 1.

F_{mult} is defined as a function of time-variant reflux rate during the thermal period or deep percolation rate above the drift ceiling after the thermal period. F_{mult} is constructed using an empirical three-parameter sigmoidal relation described in Scientific Notebook 432, Volume XII as

$$F_{mult} = \begin{cases} \frac{a}{1 + e^{\frac{\log(Q) - x_0}{b}}} & \text{if } t < t_B \\ 1 & \text{if } t > t_B \end{cases} \quad (3-1a)$$

$$Q = \left[\frac{q_r c F}{L_{WP} D_{WP}} \right] \quad (3-1b)$$

where

- a — shape parameter [dimensionless] (AFmultCoefficient in tpa.inp)
- b — scale parameter [dimensionless] (BFmultCoefficient in tpa.inp)
- x_0 — shift parameter [dimensionless] (XOFmultCoefficient in tpa.inp)
- Q — linear flux [mm/yr]
- q_r — reflux rate in the thermal period or deep percolation rate in post thermal period [m^3/yr] (Figure 2-2)
- c — conversion parameter [1000mm/m]
- F — flow focusing factor, $F_{ow} \times$ WastePackageFlowMultiplicationFactor [dimensionless]
- L_{WP} — waste package length [m] (WPLength[m] in tpa.inp)
- D_{WP} — waste package diameter [m] (WPDiameter[m] in tpa.inp)
- t_B — initial time at which rubble starts accumulating on top of the drip shield [yr]

“log” in Eq. (3-1a) refers to the common logarithm. F_{mult} is the only ambient seepage reduction factor computed internally as a function of time-variant deep percolation rate. Equation (3-1a) does not assume any specific drift geometry, and it is applicable to both intact and degraded (nominal) drift degradation scenarios. For intact drift scenario simulations, t_B is equal to the maximum simulation length. In Eq. (3-1a) the shape parameter, a, determines the maximum value of the seepage fraction; the scale parameter, b, controls the slope of the middle portion of the curve; and the shift parameter, x_0 , controls the lateral shifting of the curve.

Equation (3-1) indicates that as the entire space between the waste package and the drift wall is filled up by rubble for the degraded drift scenario, the flow reduction is assumed to be insignificant and F_{mult} is set to 1. It is postulated that the drift wall becomes an irregular surface;

thus dripping would be enhanced.

The three-parameter sigmoidal relation for $t < t_b$ is based on a Monte Carlo analysis combining the two processes of capillary diversion and along-wall seepage. Each process is represented by the sigmoidal relation in Eq. (3-1a) and separate input ranges for the Monte Carlo analysis (Figure 3-4). The input range for capillary diversion was based on the seepage model presented in Or, et al. (2005), with uncertainty derived from their choices for estimating matrix permeability. The input range for along-wall seepage is based on the assumption that along-wall flow will likely occur at low and high percolation rates. Along-wall flow will, however, dominate at low percolation rates and be minor at high percolation rates.

For each realization in the Monte Carlo analysis, parameters were first sampled for each realization. Then factors calculated using the three-parameter sigmoidal equation were multiplied, thus combining the two processes. The combined result from a large number of realizations were then fit to the equation for F_{mult} in Eq. (3-1a), first with all parameters being uncertain. This step provided mean values for a and b . The second step was to refit the Monte Carlo results using fixed values of a and b to obtain a distribution of x_o values. The distribution of x_o values shown in Figure 3-5 appears to be reasonably represented by a triangular distribution listed in Table 3-1 for the combined fitted values. Note that $x_o = 1.75$ through 1.95 were underrepresented by the triangular distribution. However, x_o values near the upper end of the probability density function predict less seepage than those at the lower end, therefore, this underrepresentation is still conservative. On the other hand, the underrepresentation of x_o near the lower end can underestimate seepage predictions, which may require a slight decrease in the mode of the distribution. However, considering the uncertainties associated with the analyses reported in this section, the mode of 1.47 (Table 3-1) is deemed reasonable for the distribution of x_o .

Table 3-1. Values of Fitting Parameters in Eq. (3-1)

Parameter	Capillary Diversion		Along-Wall Seepage		Combined
	Minimum	Maximum	Minimum	Maximum	Fitted Values
a	0.94	0.98	0.9	0.99	0.9
b	0.17	0.26	0.2	0.4	0.22
x_o	0.62	1.9	0.8	1.4	Triangular* [1,1.47,2]

*The distribution was obtained by fitting Monte Carlo results using fixed values of a and b .

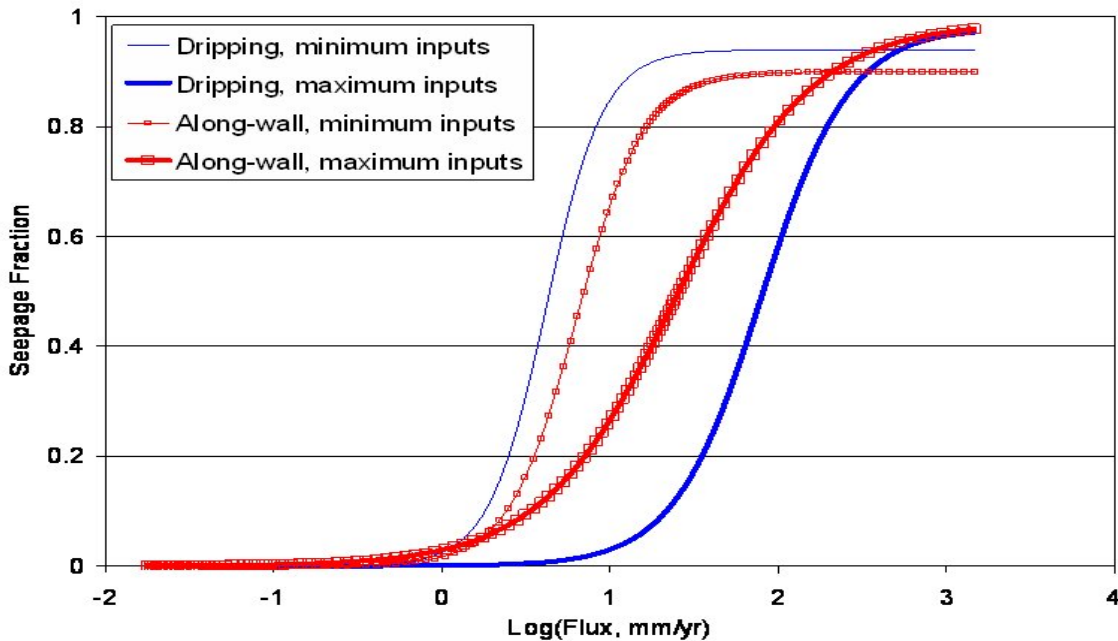


Figure 3-4. Curves Representing Minimum and Maximum Input Values in Monte Carlo Analysis for Dripping and Along-Wall Processes [1 mm = 0.039 in]

Implementation in TPA Version 5.1

The calculation of F_{mult} in TPA Version 5.1 is based on Eq. (3-1) with minor modifications and is defined as

$$F_{mult} = \begin{cases} 1 + e^{\frac{a}{\frac{\ln[Q \times c2] - x_o}{b}}} & \text{if } t < t_B \\ 1 & \text{if } t > t_B \end{cases} \quad (3-2)$$

where

c2 — Conversion factor [1 yr/mm]

“ln” in Eq. (3-2) refers to the natural logarithm. AFmultCoefficient and BFmultCoefficient were assumed to be constant to avoid complexities due to correlations among flow reduction parameters in tpa.inp. AFmultCoefficient was set a constant value of 0.9 (Table 3-1). The values for b and x_o given in Table 3-1 were multiplied by the ratio of the natural logarithm base (e) to the common logarithm base (10) in Eq. 3-2. Thus, BFmultCoefficient was set a value of 0.5. X0FmultCoefficient is sampled from a triangular distribution with the lower limit, mode, and upper limit set to 2.3, 3.4, and 4.6, respectively.

A value of the shape, scale, and shift parameters determines whether a time series of F_{mult} is

externally supplied by the user or sampled in TPA Version 5.1. If one of these parameters is negative, then TPA Version 5.1 uses either a default or a user-specified time series of F_{mult} in *wpflow.def*. This option was implemented in *ebrel.f*. Waste package length and diameter were set to a constant value of 5.165 m [16.95 ft] and 1.659 m [5.44 ft], respectively.

In TPA Version 5.1, a time series of an equivalent rubble zone diameter, eqBFB (Figure 3-6), is specified in *driftfail.dat* (generated by *driftfail* module) to account for rubble accumulation above the drip shield. It was assumed that the rubble accumulation on the drip shield occurs when the lateral gap between the drip shield and drip wall is filled up by rubble. From time zero to closure, eqBFB = 0, due to the absence of drip shield rubble. At the closure time, eqBFB is at 2.78 m [9.12 ft] and gradually increases in time to the drift diameter 5.5 m [18.04 ft] as drift degradation proceeds. The time at which eqBFB equals the drift diameter is taken as the critical time at which rubble accumulation starts on top of the drift shield. This critical time corresponds to t_b in Eq. (3-1). For intact drift simulations, t_b is set to the maximum simulation length in *exec.f*. The effect of F_{mult} can be overwritten by a factor called *SeepageThresholdT[C]* in *tpa.inp*, which will be discussed in Section 4. Equation (3-1) indicates that for $t \geq t_b$, there should not be any flow reduction from the capillary barrier effects as the capillary strength diminishes due to rubble accumulation.

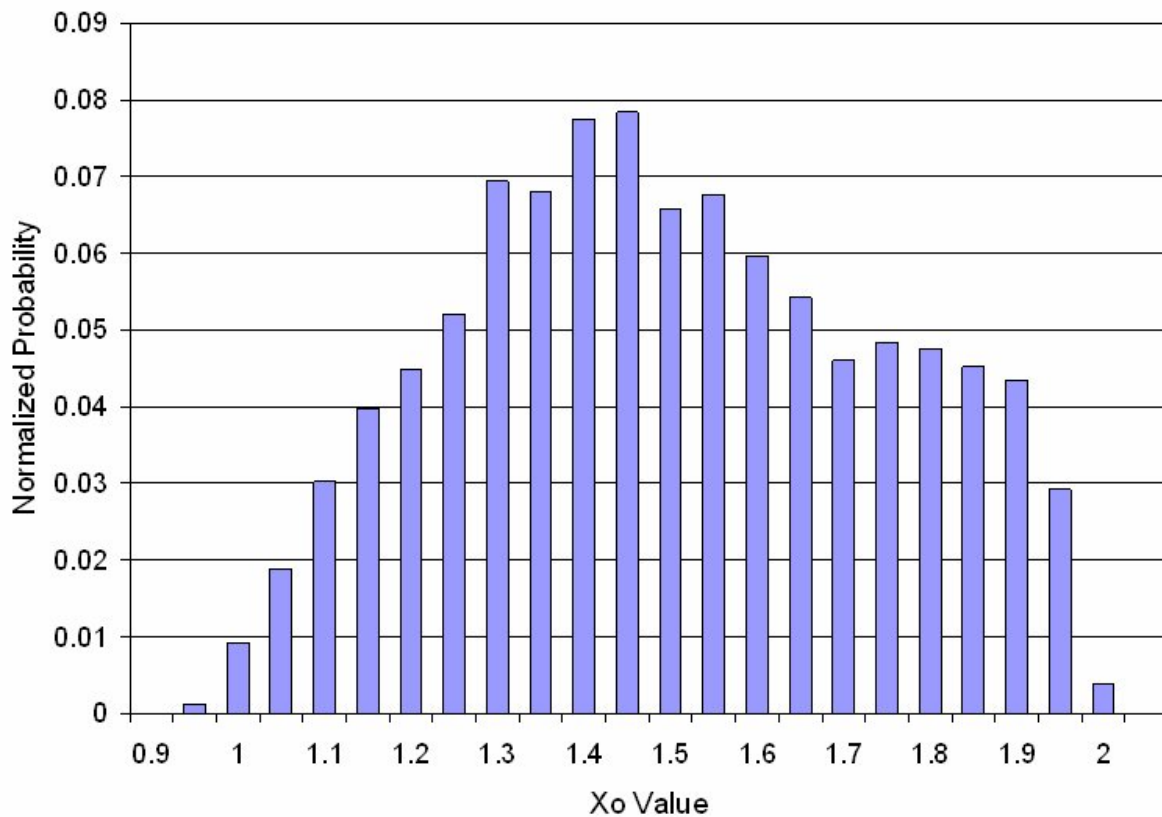


Figure 3-5. Distribution of x_o Values Derived From Monte Carlo Analysis

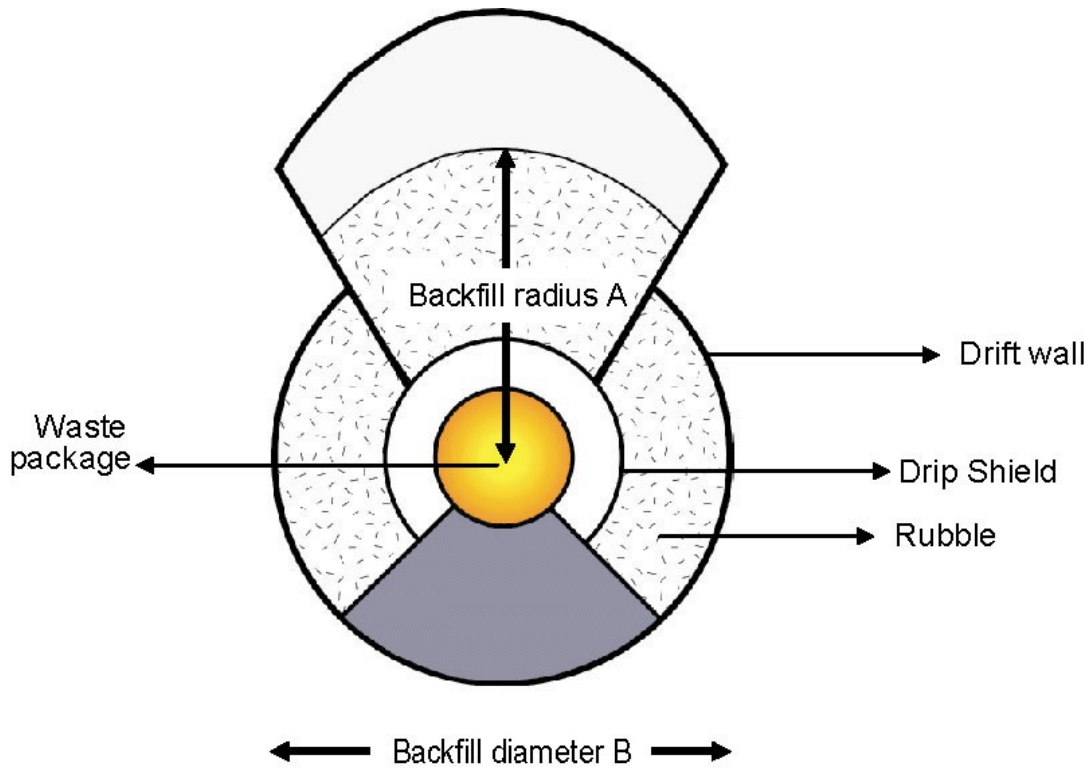


Figure 3-6. Schematic Representation of Equivalent Rubble (Backfill) Diameter Used in Eq. (3-1).

3.3. Seepage Rubble Factor, F_r

Numerical modeling of Ofoegbu, et al. (2006), supported by field observations (Figure 3-7), suggests fragments may spall from the drift crown because of thermal perturbations. Extensive spallation, or drift degradation, can also be caused by seismic events. The shape and size of fragments are affected by the orientation, intensity, length, and distribution of fractures. The shapes of initial fragments spalling from the drift wall may be affected by mechanically-induced damage in a rind around the drift, though this damage rind is believed to be small (Bechtel SAIC Company, LLC, 2004a). Ofoegbu, et al. (2006) suggest that thermally induced fragments spalling from the drift crown may continue until the drift space is filled with a rubble pile of several meters to tens of meters thick. The height of the rubble pile is dependent on the bulking factor used for the analysis. The bulking factor is a function of the fragment shape and size distribution, and the fragment packing arrangement. For understanding flow and heat transfer through the rubble, however, delineation of the shape and size distributions are important.

Rubble samples and fracture patterns were characterized from an exposure of the lower lithophysal unit of the Topopah Springs tuff on the south end of Fran Ridge, near Yucca Mountain (Figure 3-8). Analyses linked fracture characteristics to rubble fragment characteristics. This will allow translation of the Fran Ridge data to the drift and tunnel at Yucca

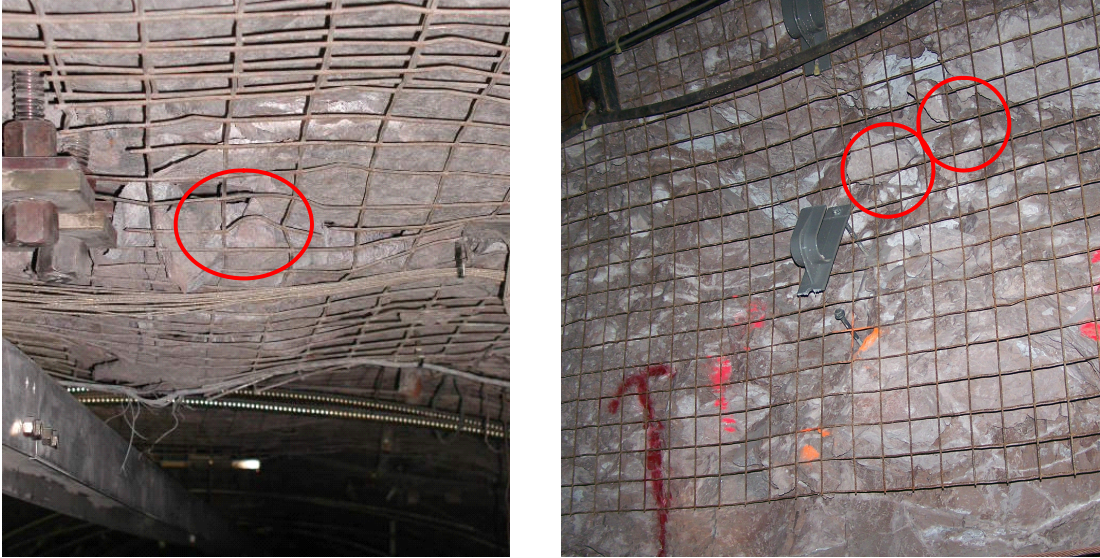


Figure 3-7. Fragments Held up by Mesh in Drift-Scale Heat Test (Left Panel); Rubble Fragment Behind Mesh in ECRB (Right Panel)



Figure 3-8. Fragments of Rubble from Analog Site at South End of Fran Ridge, Yucca Mountain

Mountain where fracture data was collected. Based on the field work and preliminary analysis of fragments from Fran Ridge, a conceptual picture of what the rubble might look like in degraded drifts has been generated. Rip-rap used for slope stability appears to be a good analogue for the rubble, in a qualitative sense. This conceptualization is consistent with spalled fragments observed in the tunnel and the contained in the mesh of the Drift-Scale Heater test (Figure 3-7). The rubble is thought to consist of a range of fragment sizes, from sand-size particles to large fragments tens of centimeters long. The volume of small particles (gravel-sized or less) is expected to be small based on observations at the Drift-Scale Heater test in April 2007 by one of the authors; a volume fraction that is too small to fill the void spaces created by the large fragments. Irregular shapes are probable, based on the fracture orientations, as supported by the fragments collected at Fran Ridge (Wyrick, et al. 2007). This characterization of the fragment shapes and sizes is necessary for understanding and predicting flow and heat transfer through a rubble pile.

Flow between coarse fragments is expected to be dominated by gravitational flow. Whereas lateral diversion of flow along variably oriented surfaces of rock fragments is expected, the scale of the rock fragment sizes compared to the scale of the drift diameter or drip shield will be an important consideration. Statistically, vertical flow is expected for the situation where fragment sizes are more than a factor of five smaller than the drift diameter. The pore sizes formed by the large fragments are likely to be too large for the capillarity-driven lateral diversion of flow.

For gravitationally dominated flow in heterogeneous media, the number of flow paths decreases with increasing depth. Flow paths that randomly meet lead to convergence of flow paths. Two sources in the literature support this concept for coarse fragment media. In the first source, Dexter (1993) analyzed flow through gravels and cobbles of various size distributions. The experiments showed that flow convergence, not divergence, occurred. A uniform distribution of flow that implies all water reaches the EBS components, whereas individual flow pathways or rivulets that converge leave the possibility that some flow pathways may not reach the EBS components. In the second source, Tokunaga, et al. (2005) used randomly packed angular rocks, obtained from Mount Diablo, California, and Arizona sandstone, in laboratory experiments to help understand flow processes in the rubble. The aggregate material was 2.5–5.0 cm [0.98–1.97 in] in diameter and fairly uniform in size. In partially saturated systems, Tokunaga, et al. (2005) experimentally observed that gravity-driven flow focuses on a smaller number of flow paths with increasing depth. At depths greater than a couple of packing layers, convergence of flow paths occurred.

Based on Tokunaga, et al. (2005) observations, the flux may focus more as the percolating water flows toward the EBS components. However, F_r is deemed highly uncertain for $t \geq t_b$ in TPA Version 5.1 because further experimental and quantitative analyses for ambient/thermal flows in partially saturated porous domains at different scales with different boundary conditions are necessary to support the experimental findings of Tokunaga, et al. (2005). Moreover, there are significant uncertainties associated with the size and shape distributions of rubble and rubble packing under different thermal and seismic conditions. It has been envisioned that the flow in the rubble is dominantly vertical, but converging flow paths in the rubble may lead to some fraction of water entering the rubble reaching the drip shield or waste package.

Implementation in TPA Version 5.1

As shown in Figure 3-9, the default value for F_r in tpa.inp is 1. The effect of rubble on the flow,

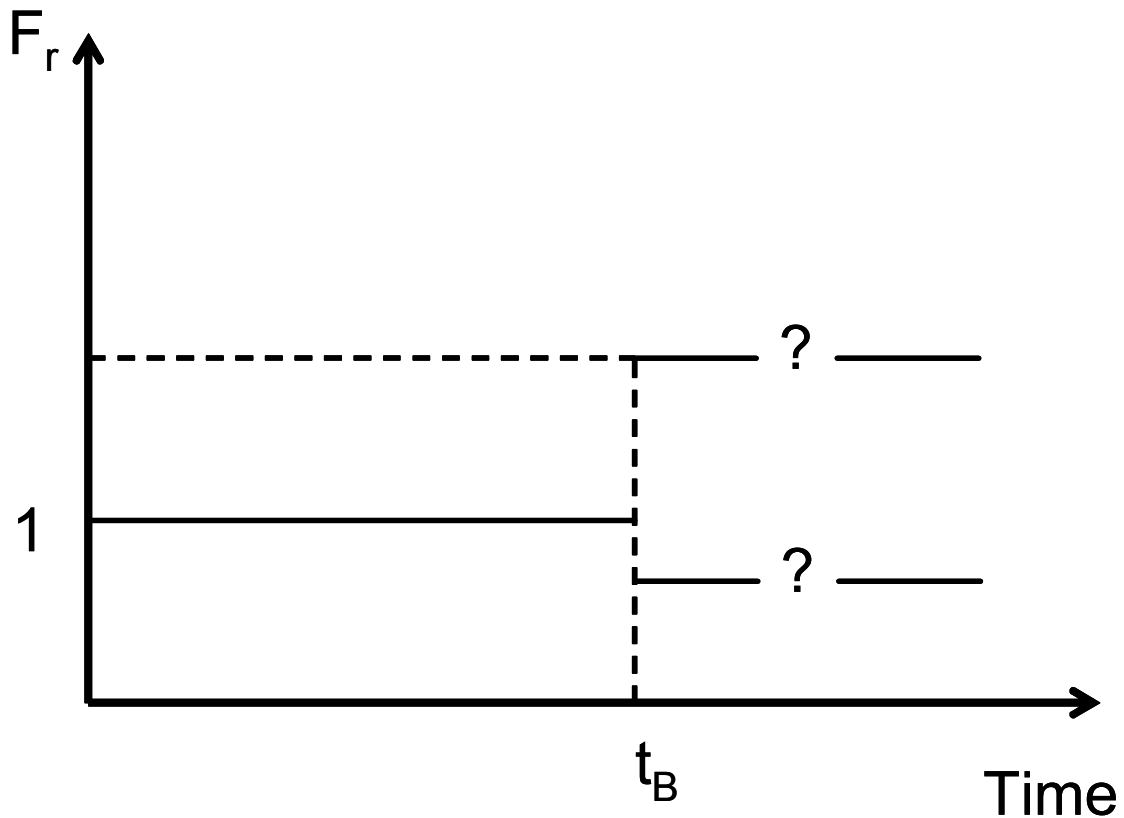


Figure 3-9. Temporal Variations in SeepageRubbleFactor, F_r .

convergence in the degraded drift remains highly uncertain because of the absence of compelling observational, experimental or numerical evidence from independent sources. Therefore, the SeepageRubbleFactor is set to 1 when the rubble is present. Flexibility in testing alternative models was an important reason for leaving the SeepageRubbleFactor in TPA Version 5.1 even though the factor was set to a value of 1. If experimental observations or numerical analyses warrant, SeepageRubbleFactor may be entered as a time-varying parameter in the auxiliary input file wflow.def.

3.4 Parameter Correlations in TPA Version 5.1

3.4.1 Guideline for Correlations

The sampling algorithm used to generate correlations among variables implemented in TPA Version 5.1 is designed to approximate Spearman rank correlations. The sampling algorithm is based on the Cholesky factorization of a covariance matrix (Helton and Davis, 2002). The Spearman rank correlation between parameters A and B is the correlation coefficient between the corresponding rank vectors. The rank vector is the collection of ranks of sampled parameter values. The rank of a parameter value is defined as the ratio of the sorted (in ascending order) position of the parameter value and the total number of elements in the parameter sample. Intuitively, a high rank correlation between A and B indicates that if the value of A is high (with

respect to the distribution function of A), then the value of B is also high (with respect to the distribution function of B). In Figure 3-10, scatter plots between parameters A and B are compared with samples constructed with different rank correlations. If rank correlations can potentially mirror expected dependencies between parameters, as a rule of thumb, those correlations should exceed 0.5 in magnitude (otherwise, proposed correlations are not clearly different from 0 as noted in Figure 3-10). Staff used Figure 3-10 as a guideline to determine the correlation strengths among the aforementioned seepage factors in the subsequent sections.

3.4.2 SubAreaWetFraction Versus WastePackageFlowMultiplicationFactor

As discussed in Section 3.1, the water that seeps from active fractures on the drift ceiling represents the maximum water flux that can potentially contact waste packages. It is conceptualized that the spacing between the active fractures (or seep points) affects the volume of water available to seep points and the fraction of waste packages that could be contacted by seepage.

As the spacing between seep points increases, seepage would occur at a smaller number of seep points at the drift ceiling. Fewer seep points would have relatively wider drainage (capture) zones covering more active fractures possibly beyond the drift footprint, which would lead to higher flow focusing (WastePackageFlowMultiplicationFactor >1). However, as the drip locations are widely spaced and the separation distance between the seep points exceeds the waste package length, some waste packages would not be contacted by seepage.

Hence, as the number of seep points on the drift ceiling decreases, the flow above the emplacement drift would be more focused (mountain-scale convergence), but the fraction of waste packages that might be contacted by seepage would be lower. This suggests an inverse correlation between WastePackageFlowMultiplicationFactor and SubAreaWetFraction. We assumed these two seepage factors are perfectly inversely correlated with a correlation strength of -0.99 . Hence, in TPA Version 5.1, WastePackageFlowMultiplicationFactor is sampled from a log-uniform distribution with bounds taken as reciprocal of the bounds for the log-uniform distribution used for SubAreaWetFraction.

3.4.3 SubAreaWetFraction Versus ArealAverageMeanAnnualInfiltrationAtStart [mm/yr]

It has been conceptualized that as the infiltration rate increases, a larger volume of water would likely reach the drift under gravity as deep percolating water. As the volume of deep percolating water increases, water in fractures near the drift ceiling would also increase and some previously dry fractures could become active and form new seep points on the drift ceiling. As the number of seep points increases, more waste packages would likely be contacted by seepage. This suggests a positive correlation between ArealAverageMeanAnnualInfiltrationAtStart[mm/yr] and SubAreaWetFraction. Use of a correlation coefficient of 0.7 reflects the uncertainty of whether a change in the deep percolation leads to a change in the number of flowing fractures or a change in the flux of flowing fractures, or both. Because SubAreaWetFraction is negatively correlated to WastePackageFlowMultiplicationFactor, WastePackageFlowMultiplicationFactor is inversely correlated with ArealAverageMeanAnnualInfiltrationAtStart[mm/yr] with a correlation strength of -0.7 .

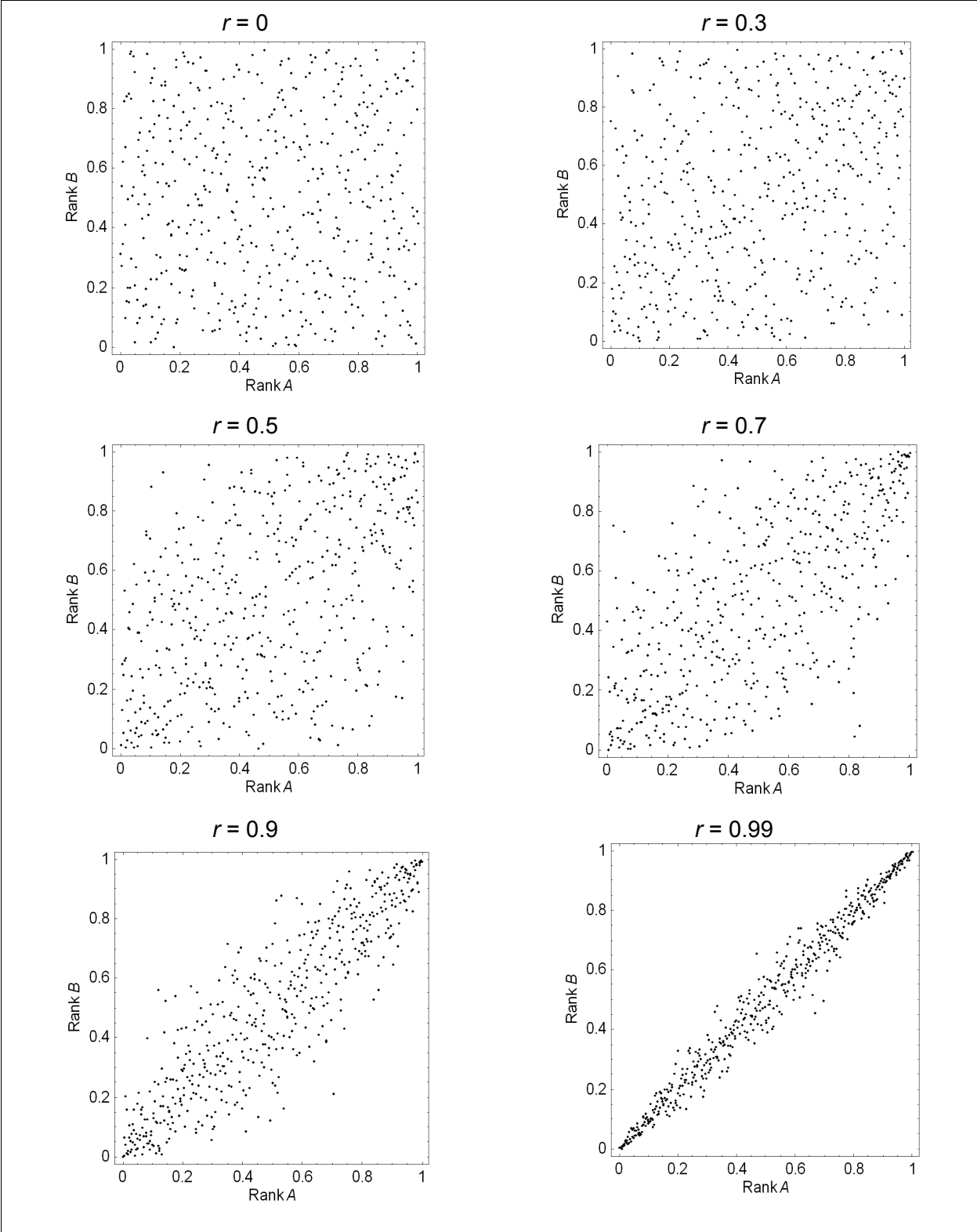


Figure 3-10. Scattered Plots of Samples Drawn With Various Spearman Rank Correlation Coefficient

3.4.4. X0FmultCoefficient Versus WastePackageFlowMultiplicationFactor

Equation 3-2 indicates that as the shift parameter, X0FmultCoefficient [x_0 in Eq. (3-1)] decreases, the seepage fraction increases for a given percolation rate, and hence the total water volume diverted at the drift opening by capillarity and water diversion on inner walls of the drift in films rivulets would decrease. This suggests that as the shift parameter decreases, more water would focus (converge) at seep points with fewer lateral diversions in the close vicinity of seep points. Therefore, the shift coefficient of F_{mult} (X0FmultCoefficient) is correlated to WastePackageFlowMultiplicationFactor with a factor of -0.9 .